

LATE MIOCEN VOLCANISM IN THE TIKVEŠ VALLEY – NORTH MACEDONIA (LOCALITY OF MRZEN)

Ivan Boev¹, Dalibor Serafimovski², Gjorgji Dimov¹

¹*Faculty of Natural and Technical Sciences, “Goce Delčev” University in Štip,
Blvd. Krste Misirkov 10-A, P.O.Box 21, 2000 Štip, N. Macedonia*

²*Faculty of Electrical Engineering, “Goce Delčev” University in Štip,
Blvd. Goce Delčev 89, 2000 Štip, N. Macedonia*

ivan.boev@ugd.edu.mk

Abstract: Late Miocene volcanism in the Tikveš Valley (MRZEN locality) is characterized by the occurrence of volcanic rocks and it is the beginning of volcanic activity in the southern parts of the Republic of North Macedonia; It occurs on the transverse tectonic structures with E-W direction that are a consequence of the extension that occurred in this region in the period of about 10 Ma (in the region of Mrzen 8.32 Ma) and which is a direct consequence of the subduction processes in the Aegean region. The chemical and geochemical characteristics of volcanic rocks indicate that these are rocks that have an intermediate character, but also contain olivine as phenocrysts, so based on that could be defined as alkaline basalts. The PEE content as well as the strontium isotopes (⁸⁷Sr/⁸⁶Sr) content range in the interval 0.706671–0.706795, while the neodymium isotopes ¹⁴³Nd/¹⁴⁴Nd range in the interval 0.512441–0.512472. Strontium isotopes (⁸⁷Sr/⁸⁶Sr) clearly indicate the origin of the primary magma from which these volcanic rocks differentiated. The source of the magma is unambiguously in the upper layer and therefore these rocks differ from the Pliocene volcanism on Kožuf Mountain where the strontium isotopes are in the range 0.7080-0.7090.

Key words: Late Miocene; volcanism; subduction; volcanic rocks

INTRODUCTION

Among the valleys in North Macedonia, the Tikveš Valley stands out in particular as a separate geographic entity with its own geomorphological and antropogeographical characteristics (Hristov et al., 1965). With an area of 2120 km², this valley occupies a substantial part of the territory of the Republic of North Macedonia. It is bounded by mountains: to the south by the Mariovo-Magelanian mountains, ranging up to the height of 1700 m. Mountain heights to the east and west are also quite high. West of the valley is mount of "Borila" at 1500 m, and to the south there are "Bali" mountain at 1400 m and "Karadak" Mt. with a height of 750 m. Limited by mountains in this way, the Tikveš Valley is cut from the Vardar river on its north side and on the west side by the Crna Reka river; the Luda Mara river passes through the middle of the valley.

From the geographical point of view, the Tikveš Valley lies on the north at the confluence of the river of Bregalnica towards the villages of Viničani and

Nogaevci, then turns over the villages of Gradsko and Dolno Čičevo, then over the villages of Sirkovo, Mrzen, Oraovec, Fariš, Raec, the village of Nikodin through the hill of Nožot to the village of Toplica. The western border of the valley starts from the Toplica area across the road Gradsko–Prilep and the villages of Raec and Drenovo towards Tikveš Lake. It covers the regions of Suva Gora with the area of the villages of Begnište, Košani and Dabnište. The south area continues over the village of Vataša, locality of Moklište, and the Vitačevo plateau. This part covers the Belgrade area with the villages of Gorni and Dolni Disan, Prždevo, and Demir Kapija. The south side ends with the village of Dren. The eastern side moves across the river of Vardar towards the village of Korešnica, cuts the Lipkovska Reka river, and goes towards the villages of Brusnik and Pepelište, crosses the Vardar river and the rail-road Skopje–Gevgelia to the village of Ulanici, and ends with the mouth of the Bregalnica river in the river of Vardar.

GEOLOGICAL AND GEOTECTONIC CHARACTERISTICS OF NORTH MACEDONIA

The geological structure of North Macedonia consists of several tectonic units that have a north-west-southeast direction within the Balkan Peninsula. The western part of N. Macedonia belongs to the Dinarides-Hellenides belt which is formed in the process of collision between the continental margin of the Adriatic and Eurasian plate (Pamić et al., 2002; Bertolotti & Principi, 2005; Zelić et al., 2010). In the central part of N. Macedonia, it is built of two tectonic units: the Pelagonides and the Vardar zone. The Pelagonides are built of highly metamorphic rocks of Precambrian age, and they extend northward to the line Scutari–Peja, i.e. Drina–Ivanjica metamorphic terrain (Marović et al., 2000; Lepitkova, 2002; Anders et al., 2006; Karamata, 2006; Schmid et al., 2008; Robertson et al., 2009). The Pelagonides are part of the passive margin of the Adriatic plate (Schmid et al., 2008). (Figure 1). The Vardar zone occupies the central part of N. Macedonia and it consists of the western ophiolitic belt (Schmid et al., 2008) or the Dinar ophiolitic sequence (Karamata, 2006) and the eastern ophiolitic belt. Within the eastern ophiolitic belt there is the Demir Kapija-Gevgelija massif, as well as the ophiolitic complex of Klepa within which the alkaline rocks of the Mrzen locality appear (Figure 1).

The eastern part of Macedonia belongs to the Serbian-Macedonian massif, which stretches from Serbia through Macedonia to Greece.

This crystalline comprises high- to medium-grade metamorphic units that were separated from

Gondwana during a Triassic rifting episode that led to the formation of a branch of the Neotethys Ocean (Vardar-Meliata Ocean) (Balogh et al., 1994; Himmerkus et al., 2002, 2009a, 2009b; Meinhold et al., 2010). They are of both MORB and subduction-related affinity (Balogh et al., 1994). The Rb/Sr and K/Ar age data suggest metamorphism during a Paleozoic orogen (48819 Ma), with Variscan and younger metamorphic overprints at 275 and 160–127 Ma, respectively (Balogh et al., 1994).

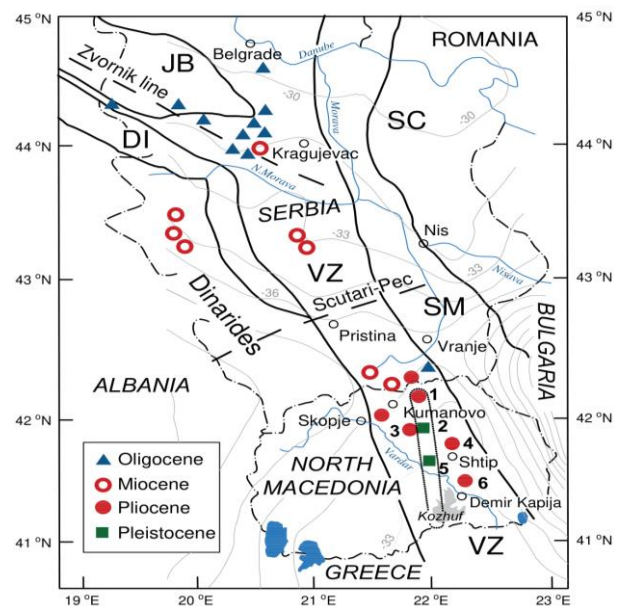


Fig. 1. Geotectonic units in the southern part of the Balkan Peninsula and the position of Neogene volcanism

GEOLOGICAL CHARACTERISTICS OF THE TIKVEŠ VALLEY

The geological characteristics of the Tikveš area were the subject of studies of many geologists, but the most complex description was given by Hristov et al. (1965). Based on these studies that were performed within the preparation of the Basic Geological Map of the Republic of Macedonia, the lito-stratigraphic sequence has the following order in the Tikveš area (Figure 2).

The oldest formations have the direction NW-SE and belong to the inner parts of the Vardar zone. The Lower Paleozoic (Pz) metamorphic complex is present with two series: amphibole and amphibole-chlorite schists with marbles, and quartz-sericite schists with marbles and phyllite layers. Serpentinite is present in the form of narrow belts along the ruptures inside the Vardar zone. The uttermost part in the SW of the Tikveš area is covered with marbles and dolomites, probably from the Devonian ages.

Over the Paleozoic-Mesozoic (Mz) formations developed, mainly of Late Cretaceous ages. The Turonian (K2) sandstones, conglomerates, and massive limestones are spread in the SW and W side of the Tikveš area. Diabase and spilite submarine flows are frequent in the lower parts of this sequence, where minor masses of gabbros occur as well. Paleozoic and Mesozoic rocks cover approximately 39 km² in the SW and W part of the Tikveš area.

Complexes of Tertiary and Quaternary sediments cover the most of the study area. The Upper Eocene (⁴E₃) flysch sediments and yellow sandstones developed along the Vardar, Crna Reka and Luda Mara valleys and the marginal part of the Tikveš basin. Those sediments with the depth up to 3500 m cover approximately 34 km², mainly in the N part of the Tikveš area.

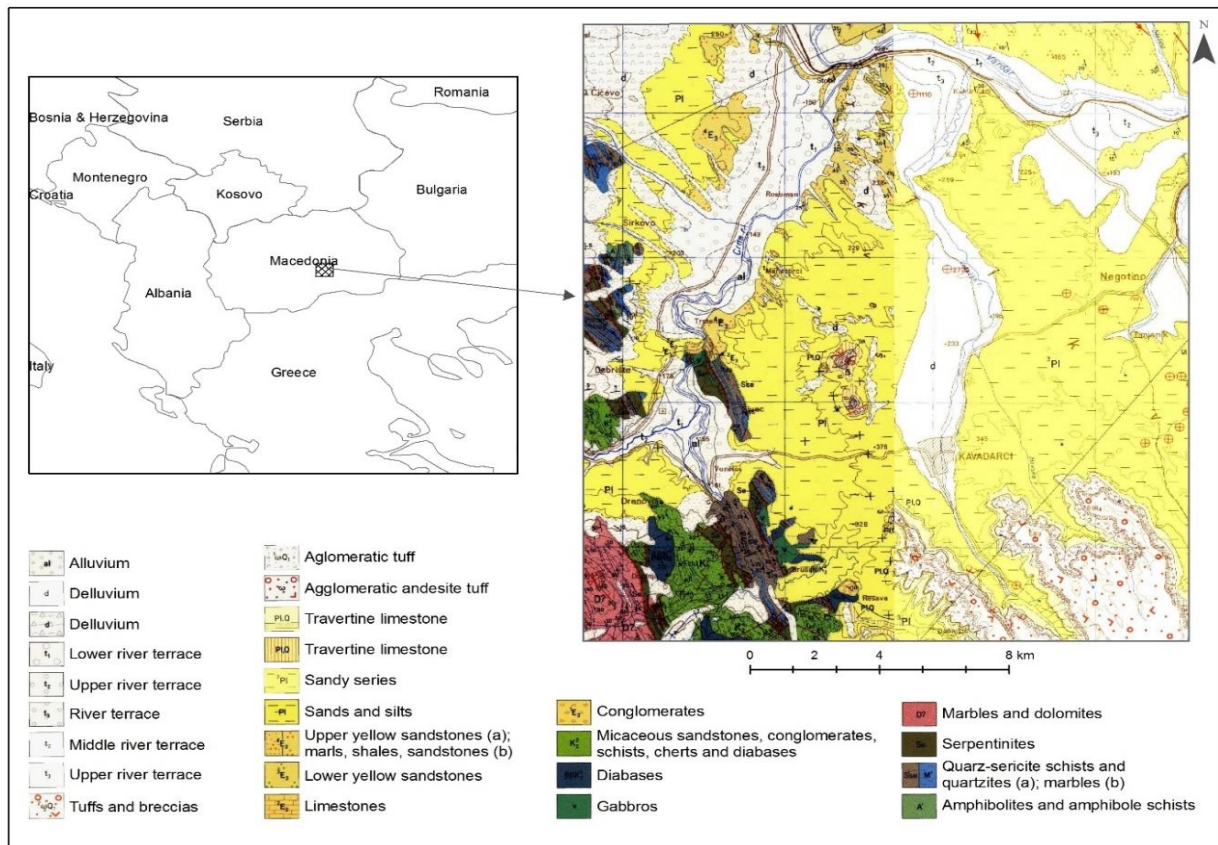


Fig. 2. Geological Map of the Tikveš Valley

Pliocene (Pl) sediments fill the Tikveš basin, limited with the Vardar river in the north, and Paleozoic-Mesozoic formations that have the direction NW-SE. This sequence is represented mainly with sandy series. The sandy series is homogeneous, it contains mostly yellow sandstone with a low percent of gravelly sandy claystone and fine-grained grey sandstone, and it is poor with fossils. Pliocene (Pl) sediments cover the biggest part (about 182 km²) in the central part of the Tikveš area.

SE from the Kavadarci, Quaternary (Q) pyroclastic volcanites are found, represented with tuffs,

breccias and agglomerates, which cover approximately 25 km².

Quaternary ages are represented with the deluvium (d), river terraces (t) and alluvium (al). Deluvial sediments (12 km²) contain rugged material from surrounding rocks, mixed with clay-sandy material. Along the rivers of Vardar, Crna Reka and Luda Mara, terrace sediments are formed (23 km²). Terraces contain gravels, sand, and clay. Alluvial sediments (40 km²) cover the flood planes of the Vardar, Crna Reka and Luda Mara rivers and contain mainly sand and clay.

NEOGENE VOLCANISM IN THE VARDAR ZONE

The central and northern part of the Balkan Peninsula was affected since Cretaceous by the NE-directed subduction, with both SW (Hellenides-Dinarides) and NE (Balkans) migrations of the orogene conjugate fronts and intervening later extension. As a result, an intricate geotectonic evolution developed, associated with magmatism with varying petrogenetic affinity ranging from calc-alkaline to alkaline or potassic. In particular, the Hellenides and Dinarides system was characterized by the occurrence of a Late Eocene-Early Miocene mag-

matic belt, expression of the Adria subduction under the Euro-Asian margin. After a time gap of 10–12 Ma (Prelević et al., 2001), the eruptive activity resumed in Late Miocene-Pliocene to Quaternary, which produced scattered volcanic centres.

In the Vardar zone in N. Macedonia and Serbia there are occurrence of potassic (P) and ultrapotassic (UP) rocks whose age ranges from Miocene (6.5 Ma) to Pleistocene (1.47 Ma) (Yanev et al., 2008) (Figure 3).

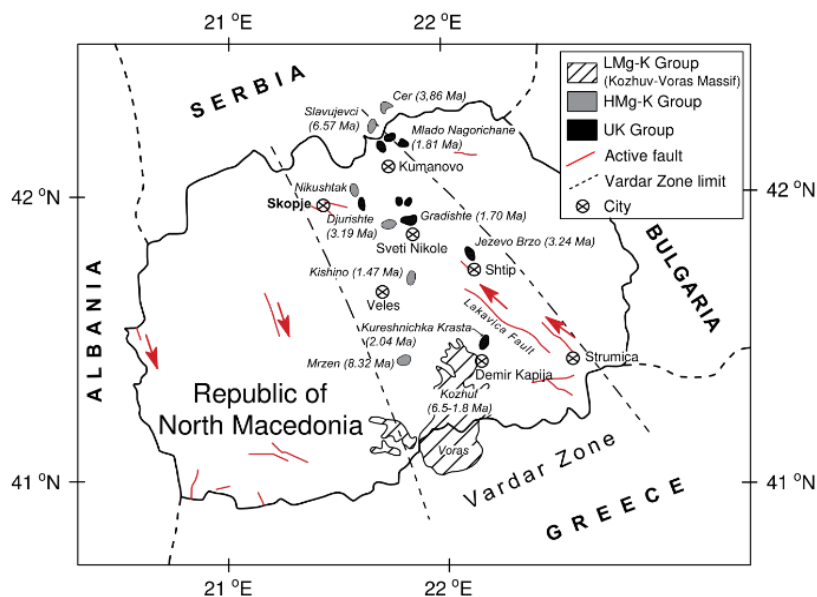


Fig. 3. Neogene volcanism in the Republic of North Macedonia

The following Cenozoic ultra and high potassic magmatic occurrences, starting from north to south, are indicated in the Vardar zone: in central Serbia, around the tectonic line of Zvornik: ultrapotassic rocks appeared on Avala, Arangelovac, Rudnik, Borac, Zabrdica, Mionica, Boljkovac and Veliki Majdan. The age of these rocks is Early Oligocene to Early Miocene (from 33,5 to 22,7 Ma, Prelevic et al., 2001; Cvetkovic et al., 2004):

- In southern Serbia, ultra-potassic rocks appear on Golija, Klinovac, and Koritnik, and high potassic rocks appear in Nova Varoš, Trebinje, Krkina Čuka, Ugljarski Krš, Vrelo, and Novi Pazar, and they have Oligocene to Late Miocene age (from 32.7 to 9.1 Ma, Prelevic et al., 2001; Cvetkovic et al., 2004).

- At the very border of Serbia with N. Macedonia (in Serbia) there are occurrences of ultrapotassic rocks, which appear along the fault zone Skutaripeja (Cvetkovic et al., 2004; Kissel et al., 1995), in the region of Devaje (21.8 Ma) and Slavujevci (6.57 Ma) and Cer (3.86 Ma) that have Miocene to Pliocene age.

- In the southern parts of N. Macedonia there is an occurrence of Miocene to Pliocene potassic rocks on Mt. Kožuf (6.5 to 1.8 Ma) and the northern parts of Greece on Mt. Voras (Kolios et al., 1980; Boev, 1988).

- Ultra-potassic rocks of Pliocene age on the territory of N. Macedonia are found in Mlado Nagorichane (1.81 Ma), Gjurište, near Sveti Nikole (3.19 Ma), Eževo Brdo in the vicinity of Štip (3.24 Ma), Kurešnička Krasta in the vicinity of Demir Kapija (2.04 Ma).

There are ultra-potassic rocks of Pleistocene age in the locality of Gradište in the vicinity of Sveti Nikole (1.7 Ma), and Kišino in the vicinity of Veles (1.47 Ma) (Yanev et al., 2008).

Within this volcanism, three different groups of rocks can be distinguished based on their geochemical affinity, as follows: the first group of rocks that has a schoshonitic affinity and these rocks appear within Mt. Kožuf (6.5 to 1.8 Ma) and they are represented by latites, trachites, quartz-latites to rhyolites (LMg-K group); the second group of rocks is represented by potassic rocks (HMg-K group) in which the ratio of K_2O / Na_2O is between 1.0 and 1.8, in N. Macedonia they occur in the area of Sv. Nikole (Gjurište) and in Cer and Slavujevci; the third group of rocks is present only on the territory of N. Macedonia and is represented by ultrapotassic rocks (UP-group), where $K_2O/Na_2O > 1.8$ and $Mg > 7.1$ are classified as ultrapotassic schoshonides (UP-latites, UP-phonotephrites, lamporoites).

Ultra-potassic volcanism in the southern parts of Serbia and N. Macedonia within the Vardar zone has been the subject of interest of many researchers (Boev, 1988; Cvetkovic et al., 2004; Boev and Yanev 2001).

This paper presents the research that has been done on a smaller volcanic body in the vicinity of the village of Mrzen (Kavadarci) and which until now has not been the subject of research. This volcanic body may represent the link between P-volcanism on Mt. Kožuf and UP-volcanism in other parts of the Vardar zone. Data on this volcanic body can be found in the paper of Molnár et al., 2021.

DESCRIPTION OF THE OCCURRENCE OF ALAKALI BASALTS AND THE GEOLOGY OF THE VICINITY

On the mountains of Kožuf and Kozjak, as well as in the southern peripheral parts of the Tikveš and Mariovo Tertiary basins, there is an occurrence of volcanic rocks that were formed during the Upper Miocene-Pliocene to the Pleistocene. These volcanic rocks appear along the transverse tectonic structures (E-W) of the Vardar stretch (NW-SE). Volcanic rocks are represented by numerous volcanic piles and volcanic necks (Kravički Kamen, Vasov Grad) as well as by the appearance of a large amount of pyroclastic rocks and lava.

The volcanic phenomena are generally located in an area with the east-west direction (E-W), but most often they are located at the intersection of tectonic structures from the Vardar direction (NW-

SE) and neotectonic structures with E-W direction. The appearance of these neotectonic structures is a result of the extension occurring during the Upper Miocene as a consequence of the subduction of the Adriatic plate below the margin of the Eurasian plate.

Exactly on such a structure in the direction of E-W south of the village of Mrzen, through the serpentine rocks, Upper-Cretaceous sediments, lake conglomerates and breccias, there is a subvolcanic magmatic body in gray-purple colour and the appearance of hollow textures. These rocks in the vicinity of the village of Debrishte are found in the form of eruptions in the conglomerates and over the conglomerates and breccias.

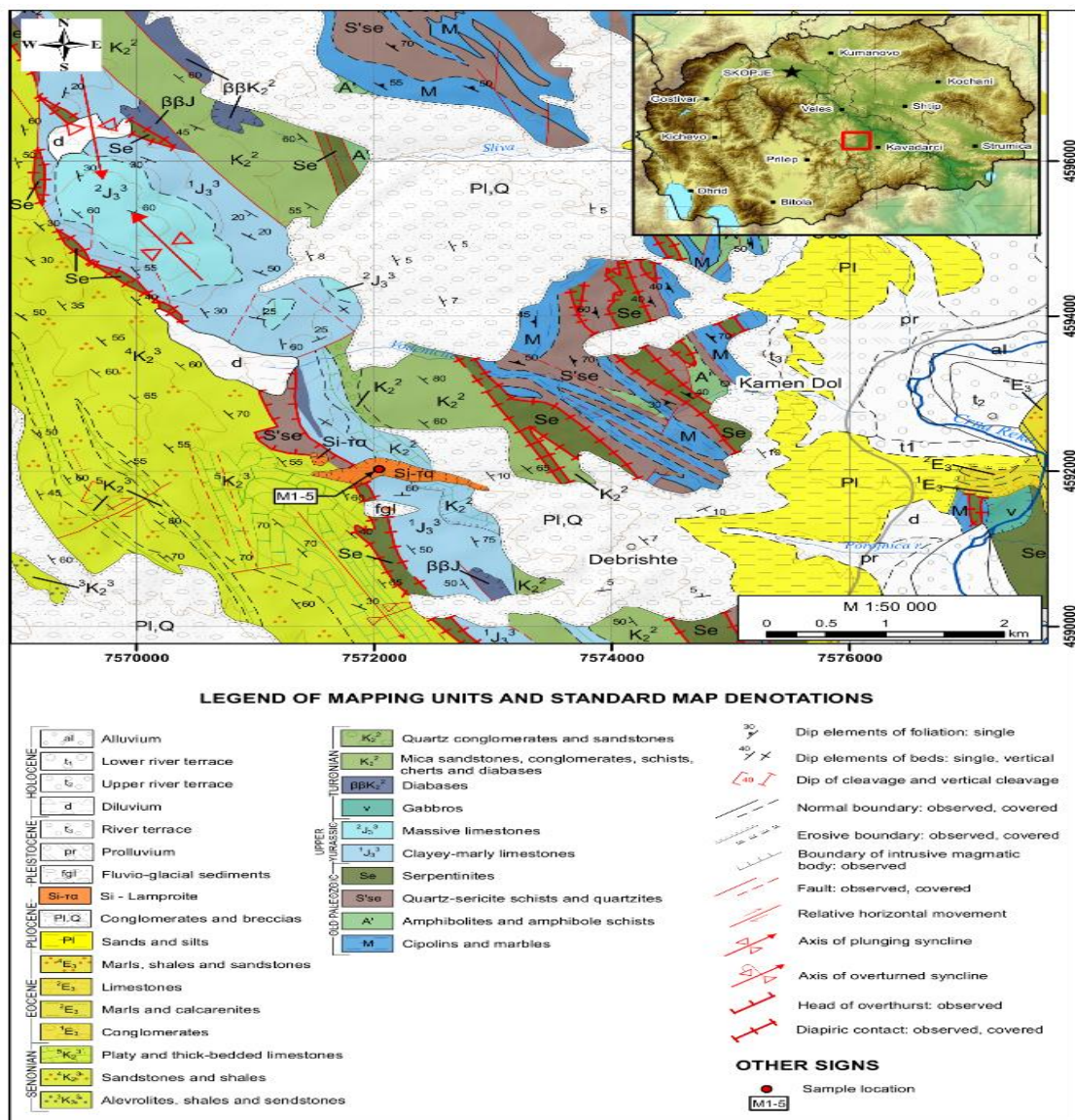


Fig. 4. Geological position of the Late Miocene volcanic body in the Tikveš Valley

Volcanic rocks appear at the intersections of this deep tectonic structure with the direction of extension (E-W) with the older structures of the Vardar direction (NW-SE). This part of the Vardar zone is represented by a series of carbonate rocks (limestones), sandstones and Cretaceous clays that appear in contact parts with a series of serpentines

and basic igneous rocks (diabases, gabbro and spilites). The series of metamorphic rocks is represented by marbles, quartz-sericite schists and quartzites, and amphibolites and amphibolite schists. The Pliocene formation is represented by sands, clays and limestones and the magmatic part is represented by alkaline basalts (Figure 4).

METHODOLOGY

Five samples were taken from the magmatic body, which were further petrographically and mineralogically processed.

Polished thin sections (PTS) were examined using a petrographic microscope, under both transmitted and reflected light. Both techniques use the properties of polarized light as it travels through, or reflects off, the mineral sample, respectively.

Within the transmitted light petrography, one can look at a sample in either 'plane polarized light' (ppl), or 'crossed polars' (xp). Plane polarized light is when the light coming through the microscope is traveling in only one direction. This state most closely resembles what the naked eye would see, just magnified. Some minerals show a slight difference in colour as the microscope stage is rotated under ppl, and this is called 'pleochroism'. It happens because the light travels faster along one of the three axial planes in the mineral compared to another. Some minerals show a high degree of pleochroism (such as amphiboles), while others are not pleochroic at all.

When a second polarizer is inserted into the light path at a right angle to the first polarizer, the incoming light is now polarized in two directions. This other polarizer is called 'analyzer', and this state is called 'crossed polars' (or 'xp' for short). The colours that we now see down the microscope are the result of the refraction of two light paths coming through the mineral, and the interaction or 'interference' between them. One light ray comes through the mineral faster than the other, and that is why the colours are called 'interference colours'. They are only seen under a petrographic microscope, and in many cases provide diagnostic information to identify minerals. When there is a large difference between the speeds of the two light rays coming out of the mineral, we can say that there is a high degree of 'birefringence', and therefore higher 'orders' of interference colours will result. This is particularly true for minerals such as carbonates that display anomalously high orders of interference colours, almost resembling a rainbow.

Opaque minerals such as sulfides and oxides appear black in transmitted light and are identified instead under 'reflected light'. This is achieved using the same petrographic microscope, in a reflected mode, where the light is now shining on the sample, instead of through it. A mineral is said to be highly 'reflective' if it appears light white or light yellow. A good example of this reflectance is arsenopyrite (white) and pyrite (light butter yellow). Other sulfides are distinguished mainly by their reflectance, from brassy yellow (chalcopyrite) to a golden yellow colour (native gold). Pentlandite has a slightly more pinkish reflectance. Oxides such as hematite and magnetite have a light grey reflectance. Silicates are usually dark grey under reflected light and only the crystal shapes and maybe cleavage traces are visible.

Specific tests are performed using both optical techniques with high powered objectives (2.5×, 5×, 10×, 20×, 50×, and 100×), and specialized petrographic accessories to identify all mineral phases present to the best of the ability of the petrographer. Note that the oculars (eyepieces) also apply a magnification of 10×, therefore the total magnification is the objective magnification multiplied by 10. Images displaying most of the pertinent mineral phases and overall textures are captured using a digital camera mounted on top of the microscope. Scale bars are included in each image, and this scale is calibrated to a micrometer prior to analysis.

Lithochemistry and whole rock analysis

The most aggressive fusion technique employs a lithium metaborate/tetraborate fusion. Fusion is performed by a robot at Actlabs, which provides a fast fusion of the highest quality in the industry. The resulting molten bead is rapidly digested in a weak nitric acid solution. The fusion ensures that the entire sample is dissolved. It is only with this attack that major oxides including SiO₂, refractory minerals (i.e., zircon, sphene, monazite, chromite, gahnite, etc.), REE and other high field strength elements are put into solution. High sulphide-bearing rocks

may require different treatment but can still be adequately analyzed. Analysis is by ICP-OES and ICP-MS.

The quality of the data is exceptional and can be used for the most exacting applications.

Electron probe micro-analyzer (EPMA)

Whenever the major and minor elements of a mineral are identified and quantified with a high precision, EPMA in-situ analyses will be the solution. Actlabs has a procedure for oxides, silicates, sulphides, and sulphates as well as alloys. EPMA analysis can be done in conjunction with MLA and QEMSCAN measurements as a complementary method.

Sr methodology

The rock powders were dissolved in HF + HNO₃ at 150 °C for 5 days, and the chemical separation procedures for Sr. Isotopic analysis for Sr used MC-ICPMS methods. All analyses are presented relative to a value of 0.710245 for the SRM987 Sr isotopic standard.

Nd methodology

Sample dissolution was performed in HF + HNO₃ at 150 °C for 5 days, and the chemical separation procedures followed Creaser et al. (1997) and Unterschütz et al. (2002) with isotopic analysis by MC-ICPMS (Schmidberger et al., 2007). Dissolution occurred in mixed ²⁴N HF + ¹⁶N HNO₃ media in sealed PFA teflon vessels at 160 °C for 6 days. The fluoride residue is converted into chloride with HCl, and Nd and Sm are separated by conventional cation and HDEHP-based chromatography. Chemical processing blanks are < 200 picograms of either

Sm or Nd and are insignificant relative to the amount of Sm or Nd analyzed for any rock sample. We analyzed the Geological Survey of Japan Nd isotope standard “Shin Etsu: J-Ndi-1” (Tanaka et al., 2000) as an unknown, which has a ¹⁴³Nd/¹⁴⁴Nd value of 0.512107 ± 7 relative to a LaJolla ¹⁴³Nd/¹⁴⁴Nd value of 0.511850, when normalized to ¹⁴⁶Nd/¹⁴⁴Nd = 0.7219. The value of ¹⁴³Nd/¹⁴⁴Nd determined for the J-Ndi-1 standard conducted during the analysis of the samples reported here was 0.512081 ± 8 (2 SE); the long-term average value is 0.512095 ± 8 [1 SD, n = 7, past year).

K-Ar methodology

An aliquot of the sample was weighed into an Al container, loaded into the sample system of extraction unit, and degassed at ~100°C over 2 days to remove the surface gases. Ar was extracted from the sample in a double vacuum furnace, at 1700°C. The determination of radiogenic Ar content was performed twice on an MI-1201 IG mass spectrometer by the isotope dilution method, with ³⁸Ar as a spike, which is introduced to the sample system prior to each extraction.

The extracted gases were cleaned using a two-step purification system. Then, pure Ar was introduced into a custom-built magnetic sector mass spectrometer (Reynolds-type). It shall be noted that the test was done twice per sample, in order to ensure the consistency of the results. Two globally accepted standards (Bern-4M Muscovite and 1/65 "Asia" rhyolite matrix) were measured for ³⁸Ar spike calibration. For age calculations, the international values for constants were used, as follows: λ_K = 0.581 × 10⁻¹⁰y⁻¹, λ_β = 4.962 × 10⁻¹⁰y⁻¹, ⁴⁰K = 0.01167 (at. %).

PETROGRAPHY AND MINERALOGY

Fine-grained laths of plagioclase and subordinate phenocrystals of clinopyroxene, olivine, probably orthopyroxene, and biotite, are randomly oriented within a very fine-grained unresolved groundmass. The fine-grained porphyritic microstructure is heterogeneously overprinted by alkali feldspar alteration (Table 1).

Alteration: alkali feldspar: moderate; iddingsite: moderate to strong after olivine

Plagioclase occurs as subhedral laths (up to 0.1 mm long), which are randomly oriented within the porphyritic microstructure. The plagioclase crystals show Albite twinnings and are relatively

fresh. In some of the laths, polysynthetic twinnings and relic growth zoning are observed. While the plagioclase laths are homogeneously distributed, and in some cases show a weak magmatic foliation, the staining colour is heterogeneous and forms small patches around some of the phenocrystals or cavities. We interpret this as evidence of the occurrence of plagioclase as fine-grained laths and the **alkali feldspar** as a very fine-grained replacement within the unresolved groundmass. This hypothesis would need to be tested by electron optic analysis.

Olivine occurs as fine-grained subhedral to anhedral phenocrystals moderately to strongly altered by iddingsitic (smectite-chlorite-goethite) products.

Table 1
Modal mineral composition of volcanic rocks
from Mrzen

Mineral	Alteration and weathering mineral	Modal %	Size range (mm)
Phenocrystals			
Olivine	Iddingsite: smectite-chlorite- goethite	3–4	up to 0.4
Clinopyroxene		2–3	up to 0.5
Orthopyroxene		1.5–2	up to 0.2
Plagioclase		59–61	up to 0.1
Alkali feldspar		30–35	up to 0.02
Magnetite		2–4	up to 0.05

Clinopyroxene forms subhedral to anhedral phenocrystals (up to 1 mm long) (Figures 5 and 5a) immersed within the fine-grained groundmass dominated by the plagioclase. The plagioclase is distinguished by its high relief, oblique extinction, and extinction angles up to 40°. In some cases, anhedral crystals showing moderate birefringence are tentatively interpreted as **orthopyroxene**, and in some cases clinopyroxene and orthopyroxene form glomerophenocrystals.

Very fine to fine-grained subhedral crystals of **magnetite** are homogeneously dispersed within the groundmass, and it is not clear if the magnetite is a primary mineral or it is an alteration mineral.

The examined rocks from the Mrzen locality have a porphyritic structure and consist of phenocrystals of olivine, pyroxene, plagioclase, magnetite which appears as an accessory mineral, as well as calcite and basic mass which by its character is microcrystalline. The chemical composition of the main phenocrystals is determined by applying the

EMPA method and the obtained results are shown in the Tables 2, 3, 4, 5, 6.

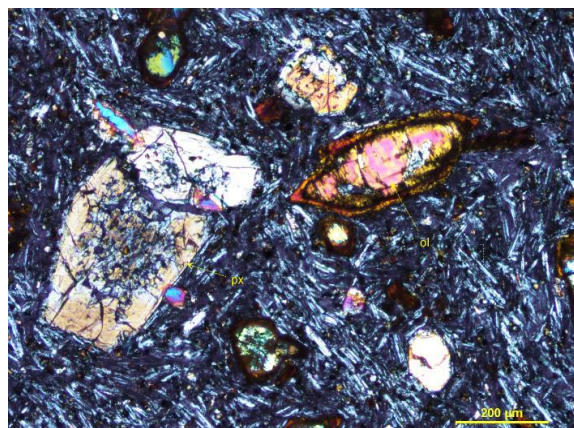


Fig. 5. Subhedral phenocrystals of pyroxene (px) and olivine (ol) are immersed within a fine-grained groundmass dominated by plagioclase (pl) and patchy aggregates of very fine-grained alkali feldspar. Crossed polarizers transmitted light.

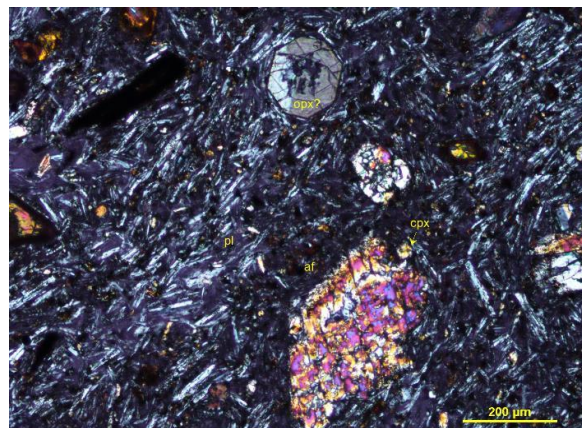


Fig. 5a. Anhedral phenocrystals of clinopyroxene (cpx) are distinguished from subhedral crystals of orthopyroxene (opx). The phenocrystals are immersed within a fine-grained groundmass of plagioclase (pl), which was overprinted by very fine-grained replacement patches of alkali feldspar (af). Crossed polarizers transmitted light.

Table 2

Selected microprobe analysis of feldspar and calculated formulae (based on 8 oxygens)

SiO ₂	64.08	64.87	62.71	57.77	64.59	65.38	64.98	65.08	64.57	62.77
Al ₂ O ₃	21.28	20.06	20.04	27.03	21.9	20.82	21.05	20.88	20.67	24.06
K ₂ O	8.24	8.79	2.86	1.09	7.24	7.64	7.01	7.82	8.42	1.47
CaO	1.64	1.53	7.62	9.92	1.88	1.29	1.24	1.9	1.3	8.22
Na ₂ O	5.25	4.79	6.73	4.65	4.24	4.21	4.47	4.86	5.43	4.45
%	100.49	100.04	99.96	100.46	99.85	99.34	98.75	100.54	100.39	100.97
Si	2.871	2.931	2.674	2.333	2.939	2.993	2.988	2.928	2.893	2.842
Al	1.124	1.068	1.007	0.954	1.175	1.123	1.141	1.107	1.092	1.284
Ca	0.079	0.074	0.348	0.429	0.092	0.063	0.061	0.092	0.062	0.399
Na	0.456	0.42	0.556	0.364	0.374	0.374	0.399	0.424	0.472	0.391
K	0.471	0.507	0.415	0.056	0.42	0.446	0.411	0.449	0.481	0.085
An	7.82	7.4	26.39	50.28	10.34	7.16	7.01	9.49	6.14	45.6
Ab	45.34	41.94	42.18	42.86	42.21	42.31	45.76	43.96	46.45	44.68
Or	46.82	50.64	31.42	6.61	47.43	50.23	47.22	46.54	47.39	9.71

Table 3

Selected microprobe analysis of clinopyroxenes and calculated formulae (based on 6 oxygens)

SiO ₂	53.49	53.46	53.35	53.24	53.29	53.45	53.14	52.83	51.61
TiO ₂	0.74	0.45	0.29	0.27	0.18	0.31	0.47	0.41	0.33
Al ₂ O ₃	3.81	2.81	2.27	2.07	2.42	2.37	3.14	2.76	2.13
Cr ₂ O ₃	0.11	0.2	0.35	0.45	0.18	0.45	0.08	0.22	0.3
FeO	7.08	5.64	4.49	4.45	4.73	4.36	5.03	5.05	4.68
MgO	11.81	15.33	17.41	17.84	17.28	17.54	15.97	16.2	18.16
MnO	0.14	0.12	0.02	0.12	0.08	0.04	0.08	0.14	0.1
K ₂ O	0.07	0.07	0.04	0.05	0.07	0.05	0.04	0.05	0.01
CaO	22.3	21.9	21.67	21.45	21.59	21.09	21.65	22.42	22.62
Na ₂ O	0.31	0.3	0.3	0.31	0.33	0.29	0.24	0.31	0.27
%	99.86	100.28	100.19	100.25	100.15	99.95	99.84	100.39	100.21
Si	2.015	1.962	1.939	1.932	1.938	1.947	1.95	1.927	1.878
Ti	0.021	0.012	0.008	0.007	0.005	0.008	0.013	0.011	0.009
Al	0.169	0.122	0.097	0.089	0.104	0.102	0.136	0.119	0.091
Cr	0.003	0.006	0.01	0.013	0.005	0.013	0.002	0.006	0.009
Fe ³	0	0	0.02	0.042	0.028	0	0	0.021	0.017
Fe ²	0.223	0.173	0.117	0.093	0.116	0.133	0.154	0.133	0.125
Mn	0.004	0.004	0.0001	0.004	0.002	0.001	0.002	0.004	0.003
Mg	0.663	0.839	0.943	0.965	0.937	0.952	0.874	0.881	0.884
Na		0.021	0.021	0.022	0.023	0.02	0.017	0.022	0.018
Ca	0.9	0.861	0.844	0.834	0.841	0.823	0.851	0.875	0.865
Wo	50.39	45.98	43.87	43.12	43.77	43.13	45.3	45.85	43.89
En	37.13	44.78	49.04	49.7	48.74	49.91	46.49	46.09	49.02
Fs	12.49	9.24	7.09	6.98	7.48	6.96	8.21	8.06	7.09

Table 4

Selected microprobe analysis of micas and calculated formulae (based on 22 oxygens)

SiO ₂	35.51	37.32	36.6	36.57	40.97	39.65	39.04	39.61	40.41	32.16
TiO ₂	1.91	2.24	2.99	2.75	2.52	2.41	4.13	2.42	2.37	2.42
Al ₂ O ₃	15.53	15.89	14.81	15.43	15.86	15.86	15.89	16.95	16.76	16.12
Cr ₂ O ₃	0.01	0.03	0.03	0	0.03	0.06	0.03	0.03	0.04	0
FeO	12.55	12.85	12.68	12.13	47.26	7.69	9.45	8.64	8.7	20.45
MgO	20.06	19.45	19.89	20.7	21.53	22.63	18.47	20.79	20.23	22.58
MnO	0.1	0	0.02	0.02	0.02	0.06	0	0.02	0.02	0.27
K ₂ O	8.77	8.19	8.51	7.98	7.66	6.78	7.7	7.52	8.46	2.18
CaO	0.19	0.09	0.18	0.16	0.08	0.31	0.17	0.18	0.02	0.42
Na ₂ O	0.57	0.4	0.76	0.6	0.38	0.24	0.67	0.213	0.53	0.37
NiO	0.1	0.01	0	0.18	0.18	0.2	0.14	0.14	0.09	0.07
%	95.3	96.47	96.47	96.52	136.49	95.89	95.69	96.513	97.63	97.04
Si	2.637	2.297	2.584	2.657	2.865	2.795	2.796	2.788	2.824	2.364
Ti	0.107	0.104	0.159	0.15	0.133	0.128	0.223	0.128	0.125	0.134
Al	1.359	1.153	1.232	1.321	1.307	1.317	1.341	1.406	1.381	1.396
Fe ³	0	0	0	0	0	0	0	0	0	0
Fe ²	0.78	0.662	0.749	0.737	0.425	0.453	0.566	0.509	0.509	1.527
Mn	0.001	0.001	0.001	0.001	0.001	0.004	0	0	0	0.017
Mg	2.221	1.785	2.093	2.242	2.245	2.378	1.972	2.182	2.108	2.474
Ca	0.015	0.006	0.014	0.012	0.006	0.023	0.013	0.014	0.001	0.033
Na	0.082	0.048	0.104	0.085	0.052	0.033	0.093	0.031	0.072	0.053
K	0.831	0.643	0.766	0.74	0.683	0.61	0.704	0.675	0.754	0.204

Table 5
Selected microprobe analysis of Fe-Ti oxides

SiO ₂	0.23	0.01	0.5	0.51	0.26
TiO ₂	8.44	9.1	10.28	8.77	8.81
Al ₂ O ₃	1.21	1.01	1.18	1.14	1.01
Cr ₂ O ₃	0.32	1.26	0.92	0.97	0.95
FeO	79.21	78.77	76.8	78.74	79.72
MnO	0.17	0.27	0.32	0.33	0.37
MgO	0.85	1.11	1.49	1.33	1.39
ZnO	0	0.08	0	0.05	0.01
NiO	0.07	0.08	0.05	0	0
Nb ₂ O ₅	0	0	0.07	0.02	0
Si	0.006	0	0.019	0.02	0.01
Ti	0.177	0.267	0.301	0.256	0.255
Al	0.04	0.046	0.054	0.052	0.046
Cr	0.007	0.039	0.028	0.03	0.029
Fe ³	1.587	1.379	1.277	1.367	1.395
Fe ²	0.257	1.194	1.223	1.188	1.173
Mn	0.004	0.009	0.011	0.011	0.012
Mg	0.922	0.065	0.086	0.077	0.08

Table 6

Selected microprobe analysis of olivines and calculated formulae (based on 4 oxygens)

SiO ₂	38.69	39.39	36.12	38.8	37.01	38.35	37.1	38.81	38.26	38.95	38.84	39.76	40.05	38.5	38.8	40.62	37.33
TiO ₂	0.01	0	0.05	0.03	0.01	0.04	0	0.15	0.18	0.1	0.12	0.07	0.17	0.14	0.08	0	0.1
Al ₂ O ₃	0.08	0.07	0.86	0	0.69	0.01	0.78	0.83	0.82	0.71	0.65	0.77	1.3	0.79	0.67	1.25	0.95
Cr ₂ O ₃	0	0.02	0.01	0.05	0.03	0.03	0.03	0	0	0	0	0	0.02	0	0	0.02	0
FeO	18.9	18.86	32.46	18.06	32.44	17.77	31.52	29	30.08	31.3	30.84	27.48	29.41	30.89	30.84	25.25	31.75
MgO	41.92	41.67	28.57	43.08	29.66	43.99	28.89	29.24	28.42	27.31	27.88	30.77	27.99	28.87	28.51	31.8	28.9
MnO	0.21	0.19	0.32	0.19	0.27	0.18	0.23	0.2	0.29	0.34	0.32	0.26	0.24	0.22	0.3	0.27	0.28
K ₂ O	0.03	0.05	0.17	0.03	0.08	0.05	0.08	0.05	0.1	0.09	0.1	0.09	0.05	0.08	0.06	0.19	0.19
CaO	0.12	0.1	1.16	0.07	0.69	0.11	0.62	0.66	2.19	0.75	0.89	0.71	0.63	1.21	0.58	0.49	0.59
Na ₂ O	0	0.04	0.06	0	0.06	0.01	0.06	0.02	0.05	0.11	0.06	0.06	0.09	0.04	0.06	0.06	0.07
NiO	0.09	0.19	0.02	0.14	0.04	0.11	0.04	0.1	0	0.08	0.06	0.1	0	0.02	0	0.15	0.01
Sum	100.05	100.58	99.8	100.45	100.98	100.65	99.35	99.06	100.39	99.74	99.76	100.07	99.95	100.76	99.9	100.1	100.17
Si	0.989	1.004	0.999	0.983	1.008	0.969	1.027	1.072	1.048	1.084	1.076	1.079	1.103	1.051	1.07	1.083	1.027
Ti	0	0	0.001	0.001	0	0.001	0	0.003	0.004	0.002	0.003	0.001	0.004	0.003	0.002	0	0.002
Al	0.02	0.002	0.028	0	0.022	0	0.025	0.027	0.026	0.023	0.021	0.025	0.042	0.025	0.022	0.04	0.031
Cr	0	0	0	0.001	0.001	0.001	0.001	0	0	0	0	0	0	0	0	0	0
Fe ³	0.02	0	0	0.032	0	0.059	0	0	0	0	0	0	0	0	0	0	0
Fe ²	0.384	0.402	0.751	0.351	0.739	0.314	0.73	0.7	0.689	0.728	0.715	0.624	0.677	0.705	0.711	0.571	0.731
Mn	0.005	0.004	0.007	0.004	0.006	0.004	0.005	0.005	0.007	0.008	0.008	0.006	0.006	0.005	0.007	0.006	0.007
Mg	1.597	1.584	1.179	1.627	1.204	1.649	1.193	1.204	1.161	1.133	1.152	1.245	1.149	1.175	1.172	1.282	1.185
Ca	0.003	0.003	0.034	0	0	0.003	0.018	0.02	0.064	0.022	0.026	0.021	0.019	0.035	0.017	0.014	0.017
Fo	79.5	79.48	59.78	80.72	61.15	81.25	61.27	63.43	62.58	59.89	60.61	65.69	64.68	61.17	61.45	68.43	61.11
Fa	20.11	20.18	38.1	18.98	37.53	18.41	37.5	35.29	37.11	38.51	37.61	32.91	34.51	36.72	37.29	30.48	37.66

PETROCHEMICAL CHARACTERISTICS

The results of the specific chemical composition of the main elements as well as the trace elements and the elements from the group of rare earths are shown in Table 7. The chemical analysis shows that these are intermediate volcanic rocks with SiO_2 content from 56.87 to 57.60% and a large amount of alkalis ($\text{K}_2\text{O} + \text{Na}_2\text{O}$) of 8.55%, of which K_2O itself ranges from 4.74 to 4.85%, so these rocks have a pronounced alkaline character. These results from

the chemical analysis indicate that these rocks could be classified as trachyandesites (Figure 6). The microscopic examinations indicate the presence of modal olivine, in an amount of about 4%, the rocks have a typical ophitic structure which changes the picture of the affiliation of these rocks, and it can be concluded that these rocks belong to the group of alkaline basalts. The normative composition of C.I.P.W. is shown in Table 8.

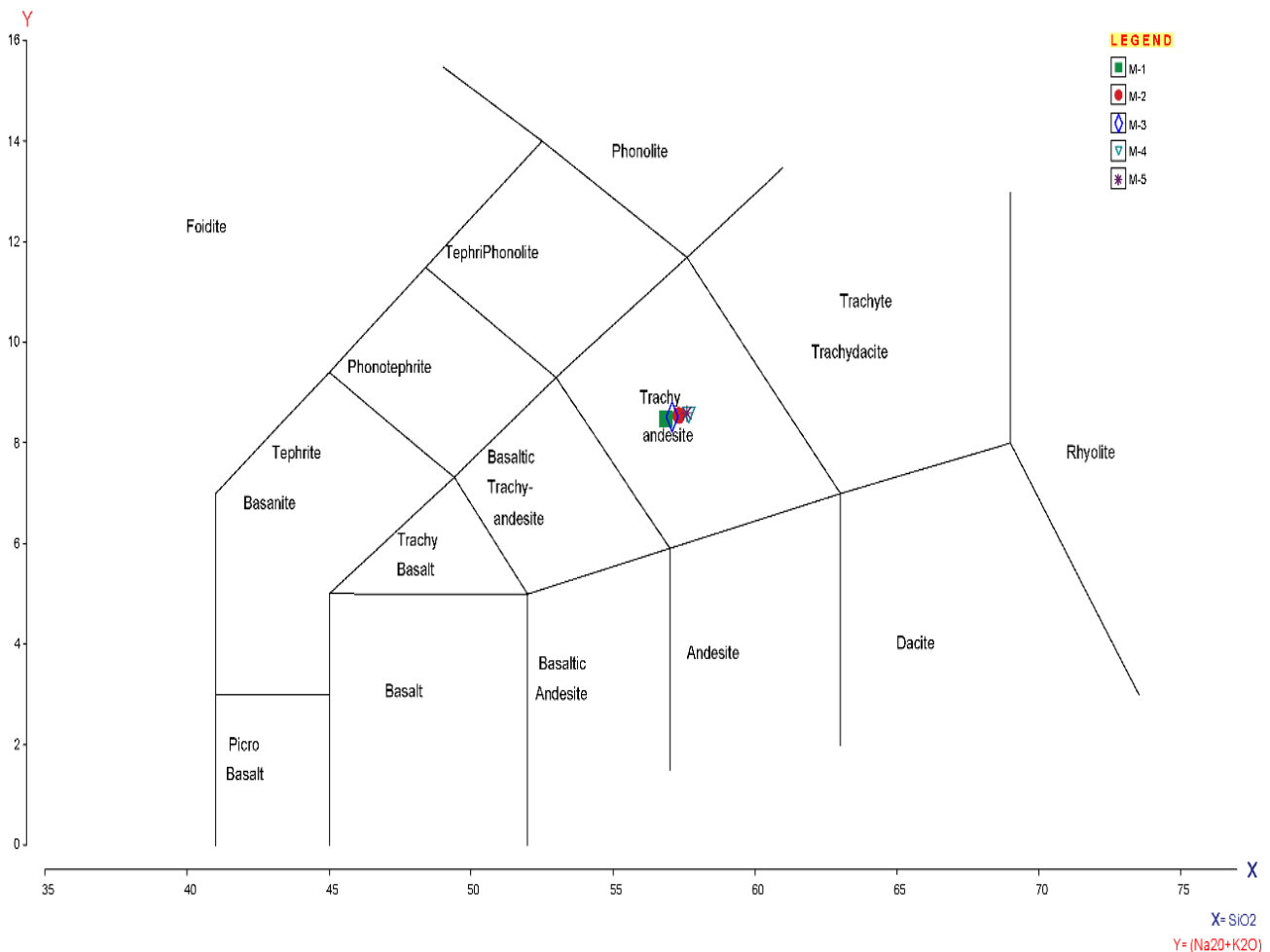


Fig. 6. TAS diagram (Le Maitre, 1989) for the Pliocene volcanic rocks near the village of Mrzen

Table 7

Chemical and geochemical composition of volcanic rocks of the Mrzen area (ICP-MS, FUS-MS)

Mineral	No of samples				
	M-1	M-2	M-3	M-4	M-5
	%				
SiO_2	56.87	57.33	57.11	57.68	57.60
TiO_2	0.997	1.006	1.015	0.986	1.005
Al_2O_3	16.7	16.55	16.50	16.45	16.83
Fe_2O_3	5.46	5.27	5.38	5.19	5.42
MnO	0.074	0.092	0.080	0.091	0.071
MgO	3.52	3.95	3.80	3.82	3.49

Mineral	No of samples				
	M-1	M-2	M-3	M-4	M-5
CaO	5.29	5.76	5.70	5.77	5.44
Na_2O	3.72	3.75	3.67	3.76	3.79
K_2O	4.74	4.80	4.85	4.78	4.79
P_2O_5	0.66	0.67	0.68	0.66	0.68
LOI	1.64	0.98	1.28	1.08	1.42
Total	99.67	100.2	100.1	100.3	100.5

Mineral	No of samples				
	M-1	M-2	M-3	M-4	M-5
	ppm				
Sc	13	12	13	12	13
Be	3	3	3	3	3
V	108	97	105	100	106
Cr	130	140	110	120	120
Co	21	22	21	22	19
Ni	80	100	110	100	90
Cu	30	40	30	30	30
Zn	50	50	60	60	50
Ga	19	20	19	18	19
Ge	0.9	0.5	1	0.9	1
As	<5	<5	<5	<5	<5
Rb	127	130	139	125	124
Sr	1143	1261	1186	1230	1169
Y	15.8	15	15.4	14.6	16.2
Zr	308	309	312	301	315
Nb	17.6	18	17.3	16.7	17.2
Mo	2	2	2	2	2
Ag	1.3	1.7	1.5	1.3	1.4
In	<1	<1	<1	<1	<1
Sn	2	1	2	2	2
Sb	<0.2	<0.2	<0.2	<0.2	<0.2
Cs	1.1	2	1.2	2.1	1.1
Ba	1571	1930	1602	1992	1580
La	51	49.9	51.4	48.3	52.6
Ce	99.6	103	106	97.4	101
Pr	12.1	11.9	12.7	11.6	12.6
Nd	44.3	43.1	45.2	41.4	44.3
Sm	6.59	6.3	6.58	6.29	6.69
Eu	1.67	1.61	1.69	1.57	1.65
Gd	3.86	4.09	3.75	3.32	3.82
Tb	0.52	0.54	0.59	0.53	0.61
Dy	2.94	2.98	3.07	2.75	3.01
Ho	0.55	0.53	0.59	0.51	0.59
Er	1.58	1.48	1.59	1.43	1.68
Tm	0.2	0.207	0.226	0.209	0.236
Yb	1.34	1.19	1.42	1.37	1.51
Lu	0.229	0.172	0.198	0.214	0.215
Hf	6.9	7.1	6.9	6.4	6.9
Ta	1.02	1.24	1.04	0.99	1.08
W	0.7	0.7	0.5	0.5	0.5
Tl	0.46	0.28	0.41	0.32	0.37
Pb	24	25	27	24	25
Bi	<0.1	<0.1	<0.1	<0.1	<0.1
Th	11.1	10	11.5	10.4	11.2
U	2.73	2.66	3.02	2.66	2.67
	%				
Q	3.90	2.98	3.32	4.04	3.96
Pl	46.35	45.88	45.28	45.71	46.83
Or	28.01	28.37	28.66	28.25	28.31
Di	3.00	5.39	5.02	4.03	3.56
Hy	7.38	7.34	7.14	7.65	7.04
Il	0.15	0.19	0.17	0.19	0.15

Mineral	No of samples				
	M-1	M-2	M-3	M-4	M-5
Hm	5.46	5.27	5.38	5.19	5.42
Ap	1.53	1.55	1.58	2.29	1.58
Sp	2.26	2.21	2.23	2.18	2.26

Table 8

Normative (C.I.P.W.) composition of the volcanic rocks from the area of Mrzen (%)

Mineral	No of samples				
	M-1	M-2	M-3	M-4	M-5
Quartz	3.9	3.7	3.9	3.6	3.5
Plagioclase	46.35	46.78	46.21	46.31	46.45
Orthoclase	28.1	27.9	28.4	28.2	28.7
Diopside	3.03	3.12	3.06	3.09	3.04
Hyperstene	7.36	7.51	7.43	7.62	7.28
Ilmenite	0.15	0.16	0.19	0.18	0.14
Hematite	5.46	5.38	5.51	5.28	5.41
Apatite	1.53	1.56	1.59	1.52	1.54
Sphene	2.21	2.23	2.45	2.31	2.28
Fe ³⁺ / (Total Fe) in rock					100.0
Mg / (Mg+Total Fe) in rock					56.1
Mg / (Mg+Fe ²⁺) in rock					100.0
Mg / (Mg+Fe ²⁺) in silicates					100.0
Ca / (Ca+Na) in rock					44.0
Ca / (Ca+Na) in plagioclase					30.8
Differentiation index					78.3
Calculated density, g/cc					2.78
Calculated liquid density					2.50
Calculated viscosity, dry					4.2
Calculated viscosity, wet					3.8
Estimated liquidus temp.					1067
Estimated H ₂ O content					1.20

The discrimination diagrams (Figure 7) show a uniform distribution of the elements shown in the correlation diagrams. This can be explained by the fact that it is a small magmatic body in which we do not have pronounced elements of differentiation, but it is a homogeneous magmatic body that is differentiated at the subvolcanic to volcanic level.

An emphasized positive correlation is seen in the discrimination diagrams of SiO₂ vs. Rb, SiO₂ vs. Ba, SiO₂ vs. Sr, as well as SiO₂ vs. Zr, which clearly speaks about the fact that we have pronounced fractional crystallization and assimilation in the primary magmatic melt.

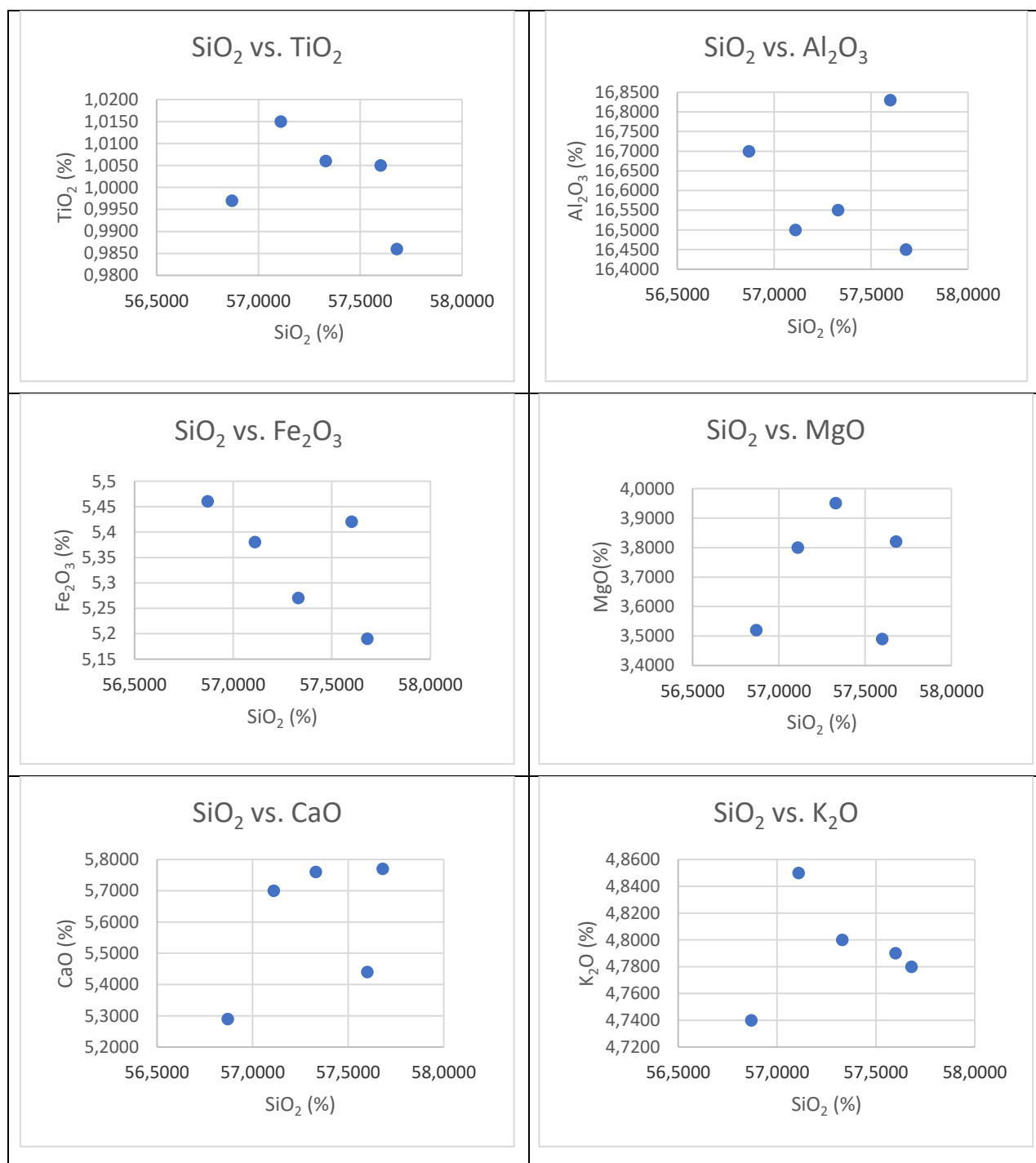


Fig. 7. Major (wt.%) and selected trace elements (ppm) vs. silica diagrams for the Mrzen volcanic rocks

GEOCHEMICAL CHARACTERISTICS

Figure 8 shows the diagram of the normalized values of REE in the volcanic rocks of the Mrzen area in terms of chondrite values (Boynton, 1984) that is characterized by significant values of enrichment LREE and MREE, relatively low HREE concentration and a low negative anomaly of Eu and Gd. It can be concluded that the amount of REE decreases with the increasing amount of SiO₂.

Figure 9 shows the diagram of the normalized values of REE in the volcanic rocks of the Mrzen area relative to the values of the primitive mantle (Sun and McDonough, 1989). From the diagram it can be seen that in all examined samples there is a significant negative anomaly of Nb, Ta and a pronounced positive anomaly of Pb.

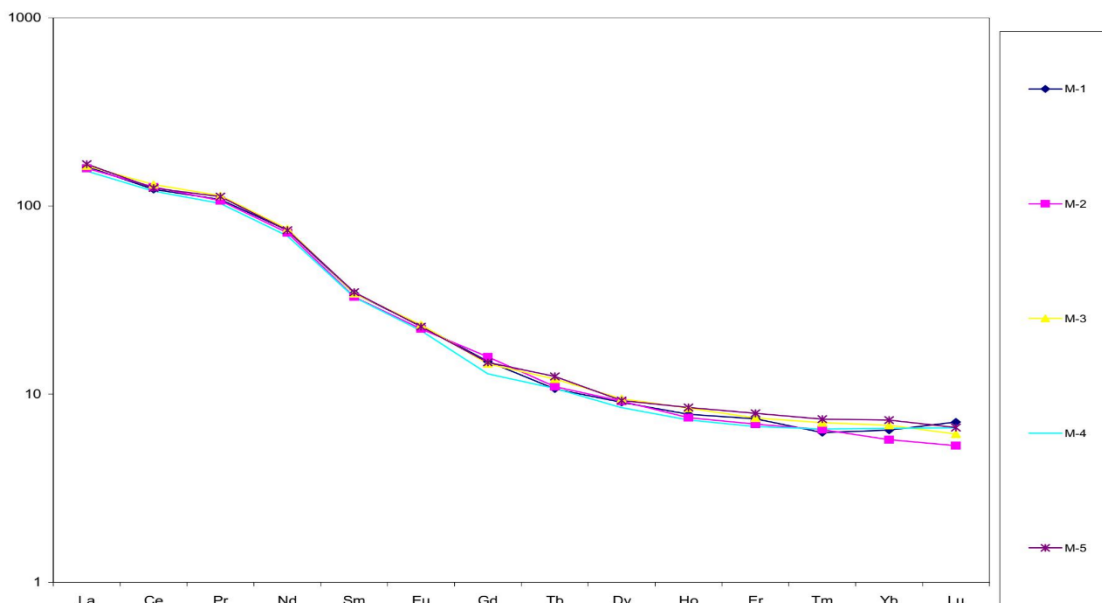


Fig. 8. Chondrite normalized REE patterns for the Mrzen volcanic rocks. Chondrite values after Boynton (1984)

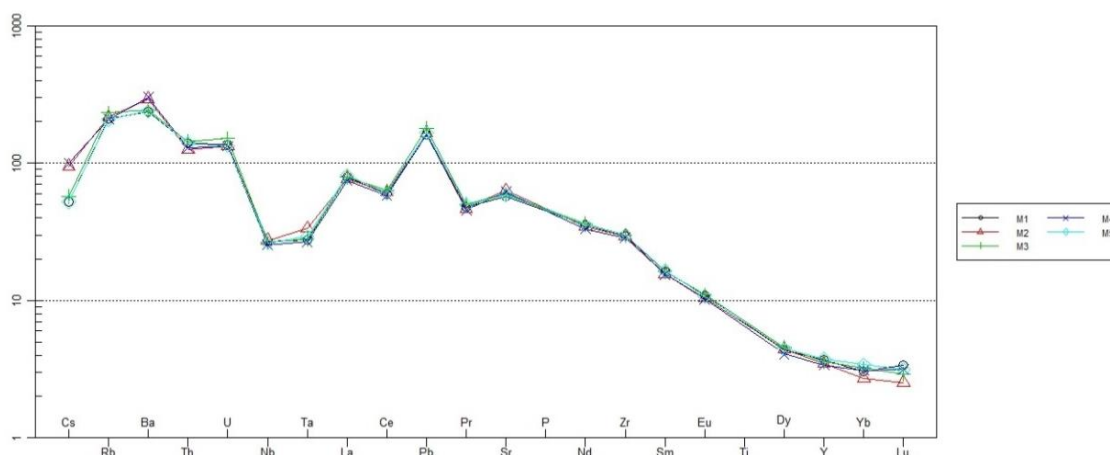


Fig. 9. Primitive mantle normalized trace elements diagram for the Mrzen volcanic rocks. Normalization factors after Sun and McDonough (1989)

Sr-Nd ISOTOPE GEOCHEMISTRY

Five analyses of the isotopes of Sr and Nd were performed, and the obtained results are shown in Table 9. The presented results show that the isotopes of strontium $^{87}\text{Sr}/^{86}\text{Sr}$ range from 0.706671 to 0.706795, while the isotopes of the neodymium $^{143}\text{Nd}/^{144}\text{Nd}$ move in the interval of 0.512441 – 0.512472. Strontium isotopes ($^{87}\text{Sr}/^{86}\text{Sr}$) clearly indicate the origin of the primary magma from which these volcanic rocks differentiated. The source of the magma is unambiguously in the upper layer and therefore these rocks differ from the Pliocene volcanism on Mt. Kožuf, where the strontium isotopes are in the interval 0.7080 – 0.7090.

Table 9

$^{87}\text{Sr}/^{86}\text{Sr}$ and $^{143}\text{Nd}/^{144}\text{Nd}$ isotope ratios in Late Miocene volcanic rocks in the Mrzen area

	$^{87}\text{Sr}/^{86}\text{Sr}$	$\pm 2 \text{ SE}$	$^{143}\text{Nd}/^{144}\text{Nd}$	$\pm 2 \text{ SE}^*$	ϵNd_0
M1	0.706776	0.000022	0.512463	0.000008	-3.4
M2	0.70671	0.000033	0.512472	0.00001	-3.2
M3	0.706795	0.000015	0.512441	0.000009	-3.8
M4	0.706772	0.000025	0.512458	0.000011	-3.5
M5	0.706766	0.00002	0.512456	0.000009	-3.6

* Uncertainty in Sr and Nd isotopic composition is ± 2 standard error.
 ϵNd_0 is the epsilon, ^{143}Nd value calculated present day

The examined volcanic rocks from the Tikveš Valley (locality of Mrzen) are characterized by low values of isotopes of $^{87}\text{Sr}/^{86}\text{Sr}$ and low isotope values of $^{143}\text{Nd}/^{144}\text{Nd}$ (Figure 10), which clearly indicates the greater similarity of these volcanic rocks with the volcanic rocks of Mt. Kožuf of Pliocene age than the rocks of the ultra-potassic volcanism in the Vardar zone. Also, from the data shown in Figure 11 it can be noticed that the examined rocks do not show any correlation between the isotopes $^{143}\text{Nd}/^{144}\text{Nd}$ and the concentration of MgO in contrast to the rocks from the Vardar zone which belong to the ultra-potassic rocks that show a pronounced correlation.

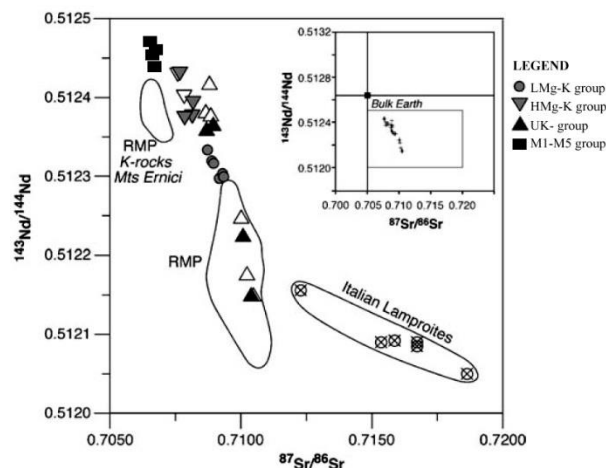


Fig. 10. $^{143}\text{Nd}/^{144}\text{Nd}$ vs. $^{87}\text{Sr}/^{86}\text{Sr}$ plot for the studied samples. The data for the Roman Magmatic Province (RMP) (Conticelli et al., 2002) and for the Tuscan lamproites (Conticelli et al., 2002; Peccerillo and Martinotti, 2006) are also plotted for comparison

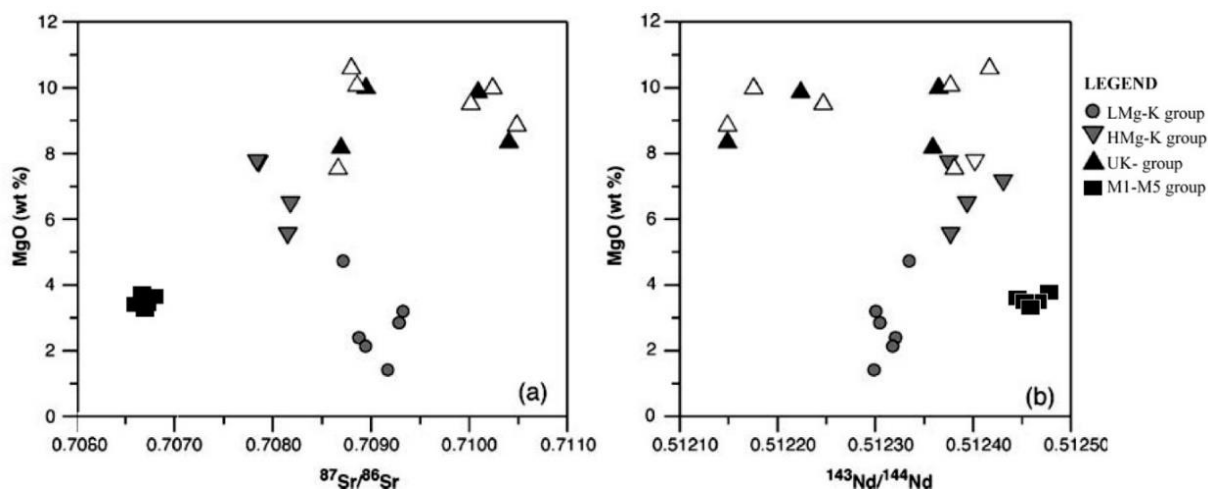


Fig. 11. MgO (wt%) vs $^{87}\text{Sr}/^{86}\text{Sr}$ (a), and MgO (wt%) vs $^{143}\text{Nd}/^{144}\text{Nd}$

K-Ar GEOCHRONOLOGY

Five analyses of the age of the volcanic rocks in the vicinity of Mrzen were performed using the method of K/Ar and the obtained data are shown in Table 10. The presented data show that the age of these rocks is Late Miocene and that these are older rocks from the volcanic rocks of Mt. Kožuf (6.5–1.8 Ma).

Table 10

K/Ar age determination of volcanic rocks from the Mrzen area

K % ± σ	^{40}Ar rad (ng/g) %	^{40}Ar air	Age Ma	Error 2σ
M1 3.98±0.04	2.250±0.007	10.9	8.32	0.18

GEODYNAMIC OBSERVATIONS

The geochemical characteristics of the examined Late Miocene volcanic rocks from the Tikveš Valley (Mrzen locality) indicate that they originate from the refractory lithospheric mantle (Cvetkovic et al., 2007) metasomatized by an agent essentially

consisting of silica melts from a subducted component already depleted in fluids. This implies that the metasomatic processes occurred during the subduction phase. This process of activation is a result of the extension processes that took place in this region

of the Balkans during Oligocene. Volcanic activity is probably the result (Figure 12) of a three-component process: 1) subduction of the Dinaride plate and the extension that is active for the Late Paleogene (Dumurdžanov et al., 2005), 2) occurrence of northwestern extension in the Aegean Sea rift, and 3) southern termination of the Panonian Basin rifting the hanging wall of the eastward retreating Carpathian subduction zone. These episodes of movement created favorable conditions for the generation of ultra-potassic to potassic magma, first in Oligocene–Early Miocene in central Serbia and later in Late Miocene–Pleistocene in southern Serbia and North Macedonia.

The position of the vulcan center of Mrzen (in the Tikveš Valley) can be clearly related to the very formation of this valley in the extension processes (Dumurdžanov et al., 2005) that took place in Late Miocene (10 Ma – 8 Ma) in the northern parts of the Aegean region. During this period, as a consequence of the subduction processes in the Aegean region, a wide zone of extension with a NS direction is formed, with the formation of the Tikveš Valley and the emergence of volcanic activity in the Mrzen region and later with the advancement of the extension processes in the south parts of the valley when it came to the formation of the mountain massif of Mt. Kožuf.

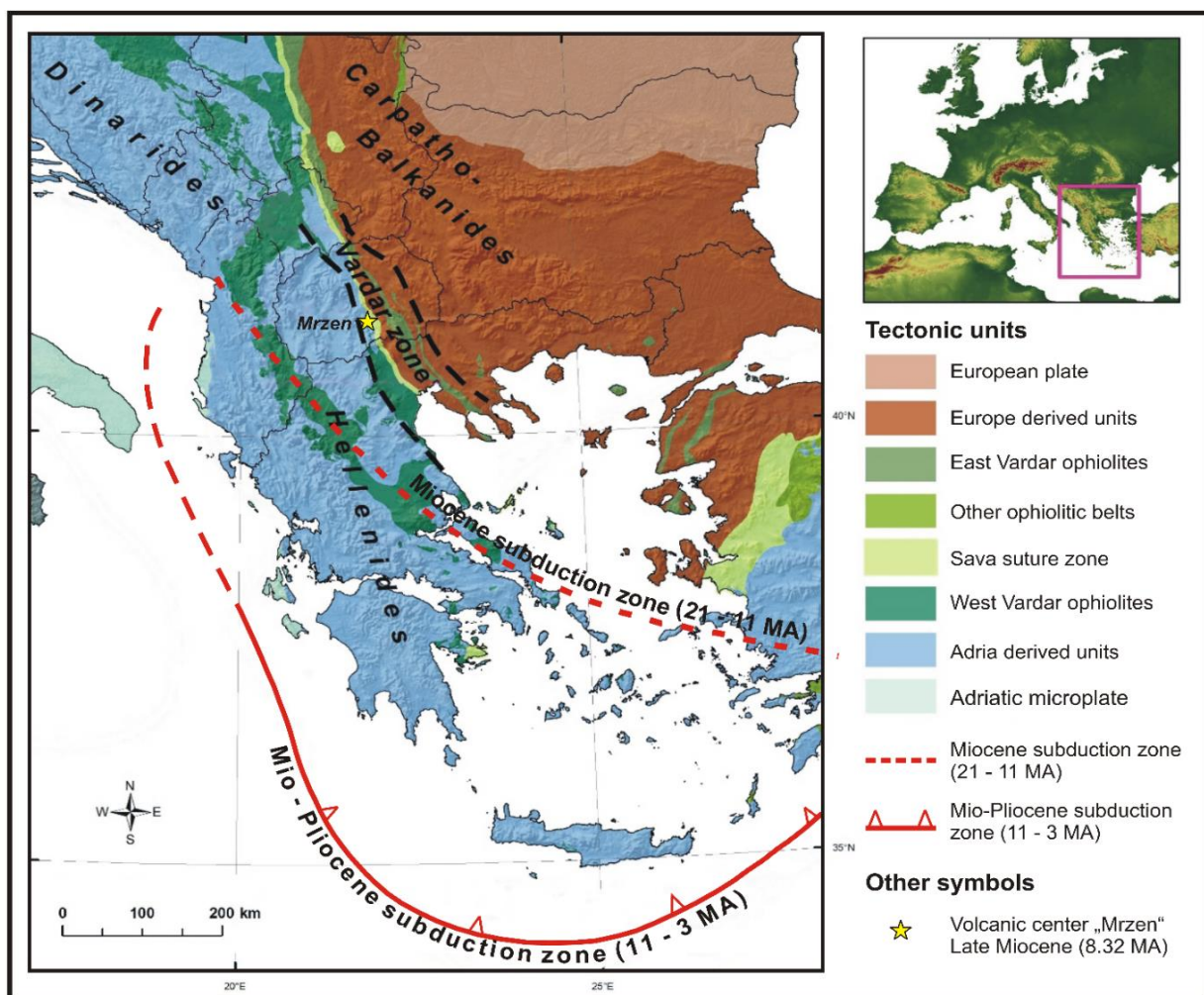


Fig. 12. Mio-Pliocene subduction zone in the Aegean region

CONCLUSION

Within the Tikveš Valley, in the area of the village of Mrzen, there are several small volcanic occurrences that are distributed on a fault structure with the E-W direction. The volcanic rocks have a

typical porphyric structure, and their texture is fluid and, in some places, there is a hollow texture. The phenocrystals in the rocks are represented by olivine, pyroxene, feldspar, and mica, while Fe-Ti

spinel appear as accessory minerals, and calcite appears as a secondary mineral. Based on chemical characteristics, these rocks can be classified in the group of intermediate rocks (trachi-andesite-latites), while based on microscopic examinations, these rocks are classified in the group of alkaline basalts.

The age of these rocks is determined as Late Miocene (8.32 Ma) and based on the geochemical characteristics, the content of REE, as well as the distribution of the isotopes of $^{87}\text{Sr}/^{86}\text{Sr}$, $^{143}\text{Nd}/^{144}\text{Nd}$, it can be concluded that these are volcanic rocks originating from the upper mantle.

REFERENCES

- Anders, B., Reischmann, T., Kostopolous, D. & Poller, U. (2006): The oldest rocks of Greece: first evidence for a Precambrian terraine within the Pelagonian zone. *Geological Magazine* **143**, 41–58.
- Balogh, K., Svingor, E. & Cvetkovic, V. (1994): Ages and intensities of metamorphic processes in the Batočina area, Serbo-Macedonian massif. *Acta Mineralogica-Petrographica* **35**, 81–94.
- Boev, B. (1988): Petrološki, geohemiski i vulkanski karakteristiki na vulkanskite karpi od planinata Kožuf [*Petrological, geochemical and volcanological features of volcanic rocks of the Kožuf Mountain – in Macedonian*]. PhD Thesis, Faculty of Mining and Geology, Štip, Ss. Cyril and Methodius University, Skopje, 195 p.
- Boev, B., Yanev, Y. (2001): Tertiary magmatism within the Republic of Macedonia, a review, *Acta Volcanologica* **13** (1–2), 57–72.
- Bortolotti, V. & Principi, G. (2005): Tethyan ophiolites and Pangea break-up. *Island Arc* **14**, 442–470.
- Boynton, W. V. (1984): Geochemistry of the rare earth elements: meteorite studies. In: Henderson P. (ed.), *Rare Earth Element Geochemistry*. Elsevier, Amsterdam, pp. 63–114.
- Conticelli, S., D'Antonio, M., Pinarelli, L., Civetta, L. (2002): Source contamination and mantle heterogeneity in the genesis of Italian potassic and ultrapotassic rocks: Sr–Nd–Pb isotope data from Roman Province and Southern Tuscany. *Mineral Petrol* **74**, 189–222.
- Creaser, R. A., Grutter, H. S., Carlson, J., Crawford, B. (2004): Macrocrystal phlogopite Rb–Sr dates for the Ekati property kimberlites: Evidence for multiple intrusive episodes during Paleocene and Eocene time. *Lithos* **76**, 399–414.
- Cvetkovic, V., Prelevic, D., Downes, H., Jovanovic, M., Vaseli, O., Pecskay, Z. (2004): Origin and geodynamic significance of Tertiary postcollisional basaltic magmatism in Srebria (central Balkan Peninsula), *Lithos* **73**, 161–186.
- Dumurdžanov N., Serafimovski T., Burchfiel, B. C. (2005): Cenozoic tectonics of Macedonia and its relation to the South Balkan extensional regime. *Geosphere* **1**, 1–22.
- Himmerkus, F., Reischmann, T. & Kostopoulos, D. (2002): First evidence for Silurian magmatism in the Serbo-Macedonian massif, northern Greece. *Geochimica et Cosmochimica Acta* **66**, A330–A330.
- Himmerkus, F., Reischmann, T. & Kostopoulos, D. (2009a): Serbo-Macedonian revisited: A Silurian basement terraine from northern Gondwana in the Internal Hellenides, Greece. *Tectonophysics* **473**, 20–35.
- Himmerkus, F., Reischmann, T. & Kostopoulos, D. (2009b): Triassic rift related meta-granites in the Internal Hellenides, Greece. *Geological Magazine* **146**, 252–265.
- Holmden, C. E., Creaser, R. A., Muehlenbachs, K. (1997): Paleosalinities in brackish water environments, A method based on the isotopic paleohydrology of strontium. *Geochimica et Cosmochimica Acta* **61**, 2105–2118.
- Hristov, C., Karajovanović, M., Stračkov, M. (1965): *Basic Geological Map of SFRJ, sheet Kavadarci, 1:100 000* (map & interpreter) Federal Geological Survey, Beograd, 62 pp.
- Karamata, S. (2006): The geological development of the Balkan Peninsula related to the approach, collision and compression of Gondwanan and Eurasian units. In: Robertson, A. H. F. & Mountrakis, D. (eds.), *Tectonic Development of the Eastern Mediterranean Region*. Geological Society, London, Special publications **260**, 155–178.
- Kissell, C., Speranza, F., Milicevic, V. (1995): Paleomagnetism of external southern and central Dinarides and northern Albanides: Implications for the Cenozoic activity of the Scurtari-Pec transverse zone, *Journal of Geophysical Research* **100**, 14999–15007.
- Kolios, N., Innocenti, F., Manetti, P., Peccerillo, A., Giuliani, O. (1980): The Pliocene volcanism of the Voras Mts (central Macedonia, Greece), *Bulletin Volcanologique* **43**, 553–568.
- Le Maitre, R. W. (1989): *A Classification of Igneous Rocks and Glossary of Terms: Recommendations of the International Union of Geological Sciences Subcommission on the Systematics of Igneous Rocks*, Blackwell, Oxford, 193 p.
- Lepitkova, S. (2002): *Petrološki, geohemiski i izotopski proučavanja na peridotitite od vnatrešniot dinarski ofiolitski pojas vo Republika Makedonija*. PhD dissertation, Ss Cyril and Methodius University of Skopje, 333 pp.
- Marović, M., Djoković, I., Pešić, L., Toljić, M. & Gerzina, N. (2000): The genesis and geodynamics of Cenozoic sedimentation provinces of the central Balkan Peninsula. *Geotectonics* **34**, 415–427.
- Meinhold, G., Kostopoulos, D., Frei, D., Himmerkus, F. & Reischmann, T. (2010): U–Pb LA–SF–ICP–MS zircon geochronology of the Serbo-Macedonian massif, Greece: Palaeotectonic constraints for Gondwana derived terranes in the Eastern Mediterranean. *International Journal of Earth Sciences* **99**, 813–832.
- Molnár, K., Lahitte, P., Dibacto, S., Benkó, Z., Agostini, S., Dönczö, B., Ionescu, A., Milevski, I., Szikszai, Z., Kertész, Z., Temovski, M. (2021): The westernmost Late Miocene–Pliocene volcanic activity in the Vardar zone (North Macedonia), *International Journal of Earth Sciences*, **111**, 749–766, <https://doi.org/10.1007/s00531-021-02153-2>.

- Pamić, J., Tomljenović, B. & Balen, D. (2002): Geodynamic and petro-genetic evolution of Alpine ophiolites from the central and NW Dinarides: an overview. *Lithos* **65**, 113–142.
- Peccerillo, A., Martinotti, G. (2006): The Western Mediterranean lamp-rotic magmatism: origin and geodynamic significance. *TerraNova*, **18**, 109–117.
- Prelević, D., Foley, S. F., Cvetković, V., Jovanović, M., Melzer, S. (2001): Tertiary ultrapotassic-potassic rocks from Serbia, *Acta Volcanologica* **13** (1–2), 101–115.
- Robertson, A., Karamata, S. & Saric, K. (2009): Overview of ophiolites and related units in the Late Palaeozoic–Early Cenozoic magmatic and tectonic development of Tethys in the northern part of the Balkan region. *Lithos* **108**, 1–36.
- Schmid, S., Bernoulli, D., Fügenschuh, B., Matenco, L., Schefer, S., Schuster, R., Tischler, M. & Ustaszewski, K. (2008): The Alpine-Carpathian-Dinaridic orogenic system: Correlation and evolution of tectonic units. *Swiss Journal of Geosciences* **101**, 139–183.
- Schmidberger, S. S., Heaman, L. M., Simonetti, A., Creaser, R. A., Whiteford, S. (2007): Lu-Hf, in situ Sr and Pb isotope and trace element systematics for mantle eclogites from the Diavik diamond mine: Evidence for Paleoproterozoic subduction beneath the Slave craton, Canada. *Earth and Planetary Science Letters* **254**, 55–68.
- Sun, S. S., McDonough, W. F. (1989): Chemical and isotopic systematics of oceanic basalts implications for mantle composition and processes. In: Saunders A.D., Norry M.J. (eds.) *Magmatism in the Ocean Basins*. J Geol Soc, London Spec Publ, **42**, 313–345.
- Tanaka, T., et al. (2000): JNdi-1: a neodymium isotopic reference in consistency with LaJolla neodymium. *Chemical Geology* **168** (3–4) 279–281.
- Unterschutz, J. L. E., Creaser, R. A., Erdmer, P., Thompson, R. I., Daughtry, K. L. (2002): North American margin origin of Quesnel terraine strata in the southern Canadian Cordillera: Inferences from geochemical and Nd isotopic characteristics of Triassic metasedimentary rocks. *Geological Society of America Bulletin* **114**, 462–475.
- Yanev, Y., Boev, B., Manetti, P., Ivanova, R., D’Orazio, M., Innocenti, F. (2008): Mineralogy of the Plio-Pleistocene potassic and ultrapotassic volcanic rocks from the Republic of Macedonia, *Geochemistry, Mineralogy and Petrology* **46**, 35–67, Sofia.
- Zelić, M., Marroni, M., Pandolfi, L. & Trivić, B. (2010): Tectonic setting of the Vardar suture zone (Dinaric-Hellenic belt): The example of the Kopaonik area (southern Serbia). *Ofoliti* **35**, 49–69.

Резиме

ДОЦНОМИОЦЕНСКИ ВУЛКАНИЗАМ ВО ТИКВЕШКАТА КОТЛИНА
(СЕВЕРНА МАКЕДОНИЈА, ЛОКАЛИТЕТОТ МРЗЕН)Иван Боев¹, Далибор Серафимовски², Ѓорѓи Димов¹¹Факултет за природни и технички науки, Универзитет „Гоце Делчев“ во Штип,

Бул. „Крсте Мисирков“ 10-А, б, факс 21, 2000 Штип, С. Македонија

²Електротехнички факултет, Универзитет „Гоце Делчев“ во Штип,

Бул. „Гоце Делчев“ 89, 2000 Штип, С. Македонија

ivan.boev@ugd.edu.mk

Клучни зборови: доцен миоцен; вулканизам; субдукција; вулкански карпи

Доцномиоценскиот вулканизам во Тивешката Котлина (локалитетт Мрзен) се карактеризира со појава на вулкански карпи, кои истовремено го означуваат и почетокот на вулканската активност во јужните делови на Република Северна Македонија. Овој вулканизам се појавува на трансверзалните тектонски структури со И-З протегање, кои се последица на екстензијата која се случила во овој регион во периодот пред околу 10 милиони години (Ma) (во реонот на Мрзен 8,32 Ma), а која е директна последица на процесите на субдукција во егејскиот регион. Деталните микроскопски испитувања на 5 примероци од вулканските карпи покажуваат дека тие имаат типична порфирска структура, додека текстурата е трахитска. Фенокристалите се идиоморфни и се претставени со: оливин, клинопироксен, ортопироксен, плагиоклас и магнетит. Има појава на алтерации на фенокристалите, при што се појавуваат следните минерали: идингсит (смеса од смектит-хлорит и гетит), минерали на глина, зеолити и калцит. Основната маса е хипокрис-

талеста, а наместа и стаклеста. Хемиските и геохемиските карактеристики на вулканските карпи укажуваат на тоа дека станува збор за карпи кои имаат интермедијарен карактер, но во модалниот состав на карпата се појавува и оливин во вид на фенокристали, и на основа на тоа би можело овие карпи да се дефинираат како алкални базалти. Содржината на изотопите на стронциумот $^{87}\text{Sr}/^{86}\text{Sr}$ се движи во интервалот од 0,706671 до 0,706795, додека изотопите на неодиумот $^{143}\text{Nd}/^{144}\text{Nd}$ се движат во интервалот од 0,512441 до 0,512472. Изотопите на стронциумот ($^{87}\text{Sr}/^{86}\text{Sr}$) јасно укажуваат на потеклото на примарната магма од која се диференцирале овие вулкански карпи. Изворот на магмата е недвосмислено во горната обвивка (upper mantle) и по тоа овие карпи се разликуваат од плиоценскиот вулканизам на планината Кожуф каде изотопите на стронциумот се во интервалот од 0.7080 до 0.7090 и изворот на магматитите се лоцира на граничното подрачје на горната обвивка и долните делови на континенталната кора.